IEICE TRANS. COMMUN., VOL.E87–B, NO.3 MARCH 2004

PAPER Special Section on Internet Technology IV

A Study on Performance of Hierarchical Mobile IPv6 in IP-Based Cellular Networks

Sangheon PACK[†a)] ***and*** **Yanghee CHOI**[†], ***Nonmembers***

SUMMARY Next-generation wireless/mobile networks will be IP-based cellular networks integrating Internet with the existing cellular networks. Recently, Hierarchical Mobile IPv6 (HMIPv6) was proposed by the Internet Engineering Task Force (IETF) for efficient mobility management. HMIPv6 reduces the amount of signaling and improves the performance of MIPv6 in terms of handoff latency. Although HMIPv6 is an efficient scheme, the performance of wireless networks is highly dependent on various system parameters such as user mobility model, packet arrival pattern, etc. Therefore, it is essential to analyze the network performance when HMIPv6 is deployed in IP-based cellular networks. In this paper, we develop two analytic models for the performance analysis of HMIPv6 in IP-based cellular networks, which are based on the random-walk and the fluid-flow models. Based on these analytic models, we formulate the location update cost and the packet delivery cost. Then, we analyze the impact of cell residence time and user population on the location update cost and the packet delivery cost, respectively. In addition, we study the variation of the total cost as the session-to-mobility ratio is changed and the optimal MAP domain size to minimize the total cost is also investigated.

key words: *Hierarchical Mobile IPv6, performance analysis, analytic model, random-walk model, fluid-flow model*

1. Introduction

In wireless/mobile networks, users freely change their service points while they are connected. In this environment, mobility management is an essential technology for keeping track of the users' current location and for delivering data correctly. In terms of cellular networks for voice call services, many schemes have been proposed to provide efficient mobility management [1]. However, since next-generation wireless/mobile networks will be unified networks based on IP technology, they will have different characteristics from the existing cellular networks. Therefore, the design of IP-based mobility management schemes has become necessary.

The Mobile IP working group [2] within the Internet Engineering Task Force (IETF) proposed a mobility management protocol, called Mobile IPv4 [3]. Mobile IPv4 allows the transparent routing of IP packets to mobile nodes (MNs) connected to the Internet. Each MN is always identified by its home address, regardless of its current point of attachment to the Internet. While it is located away from its home network, the MN is also attributed a care-of address (CoA) which provides information about its current point of attachment to the Internet. Generally, the CoA indicates the address of a foreign agent (FA) as an end point for packet tunneling. The Mobile IP provides for the possibility of registering the CoA with a home agent (HA). The HA sends packets destined for the MN through a tunnel to the CoA. After arriving at the end of the tunnel, each packet is decapsulated and then delivered to the MN.

However, Mobile IPv4 is not a suitable solution for environments in which MNs frequently change their points of attachment to the network, in other words the so-called *micro-mobility environments*. Also, since all data packets have to transit via the limited number of nodes, which make up the FAs and HAs, basic Mobile IPv4 is not scalable. To overcome these drawbacks, the Mobile IPv6 (MIPv6) protocol was proposed by the Mobile IP Working Group [4].

Mobile IPv6 allows an MN to move within the Internet topology while maintaining connections between the MN and correspondent nodes (CNs). To do this the MN sends Binding Update (BU) messages to its HA and all CNs every time it moves. Authenticating the BU message requires approximately 1.5 round trip times between the MN and each CN. These round trip delays disrupt active connections each time a handoff to a new access router (AR) is performed. Eliminating this additional delay element from the time-critical handoff period provides the improved performance with Mobile IPv6. Moreover, in the case of wireless links, it is required to reduce the number of messages sent over the air interface to all CNs and to the HA. Thus, the existence of a local anchor point allows Mobile IPv6 to benefit from reduced mobility signaling with external networks.

Hierarchical Mobile IPv6 (HMIPv6) [6] is an enhanced Mobile IPv6 to minimize the signaling cost using a local agent called Mobility Anchor Point (MAP). The MAP can be located at any level in a hierarchical network of routers, including the AR. The MAP is intended to limit the amount of Mobile IPv6 signaling outside the local domain.

An MN entering a MAP domain will receive Router Advertisements containing information on one or more local MAPs. The MN can bind its current CoA (on-link CoA (LCoA)) with an address on the MAP's subnet (regional CoA (RCoA)). Acting as a local HA, the MAP receives all packets on behalf of the MN it is serving and encapsulates and forwards them directly to the MN's current address. If the MN changes its current address within a local MAP domain, it only needs to register the new address with the MAP. Hence, only the RCoA needs to be registered with the CNs and the HA. The RCoA does not change as long as the MN moves within the same MAP domain. This makes the MN's mobility transparent to the CNs it is communicating

Manuscript received June 23, 2003.
Manuscript revised September 8, 2003.
[†]The authors are with Seoul National University, Seoul, Korea.
a) E-mail: shpack@mmlab.snu.ac.kr

with. A MAP domain's boundaries are defined by means of the ARs advertising the MAP information to the attached MNs.

Recently, Xie et al. proposed an analytic model for Mobile IP regional registration [5] which is a kind of hierarchical mobility management scheme [7]. The proposed analytic model focused on the determination of the optimal size of regional networks, given the average total location update and packet delivery cost. In this study, Xie et al. assumed the existence of one-level regional networks where there is only one Gateway Foreign Agent (GFA). Also, Woo proposed an analytic model to investigate the performance of Mobile IP regional registration [8]. In [8], Woo measured the registration delay and the CPU processing overhead loaded on the mobility agents to support regional registration. The analytic model proposed in [8] is based on the fluid-flow mobility model.

Although these models are well-defined analytic models, they have some drawbacks. First, they are based on Mobile IPv4 and not Mobile IPv6. Furthermore, [7] used a spatial-oriented Internet architecture for performance analysis. Currently, the Internet is based on the spatial-oriented location area model, which specifies that the distance between two end points situated on the Internet has nothing to do with the geographic locations of these two points. However, the ARs used in next-generation wireless/mobile networks may utilize a cellular architecture to maximize the utilization of the limited radio resources. Therefore, it is more appropriate for us to analyze network performance in context of IP-based cellular networks. Besides, [8] considered only the fluid-flow mobility model. Although the fluid-flow model is suitable for modeling of users with a high mobility, it is not appropriate to model pedestrian users. In general, random-walk model is widely used for modeling of pedestrian mobile users.

In this paper, we propose two analytic models for HMIPv6, which can be used to evaluate its performance in terms of location update and packet delivery. We assume wireless IP networks with a hexagonal cell structure and the proposed analytic models are based on both the random-walk model and the fluid-flow model. The remainder of this article is organized as follows. In Sect. 2, we propose two analytic models based on the random walk and fluid-flow mobility models. Section 3 formulates the location update cost and the packet delivery cost using the analytic models. Section 4 presents various numerical results which show the impacts of the cell residence time, user population, and MAP domain size on the location update and packet delivery costs. Section 5 concludes this paper.

2. Analytic Mobility Model

This paper assumed an hexagonal cellular network architecture, as shown in Fig. 1. In addition, each MAP domain is assumed to consist of the same number of rings, R. Each ring r ($r \geq 0$) is composed of $6r$ cells. The innermost cell 0, is called the center cell. The cells labeled 1 formed the first ring around cell "0," the cells labeled 2 formed the second ring around cell 0 and so forth. Therefore, the number of cells up to ring R, $N(R)$, is calculated using the following equation:

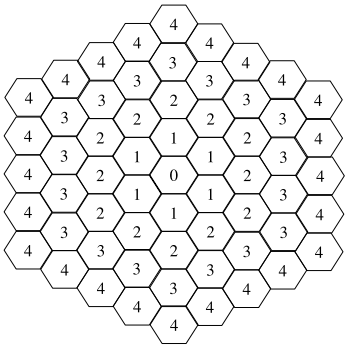

Fig. 1 Hexagonal cellular configuration in HMIPv6 architecture.

$$N(R) = \sum_{r=1}^{R} 6r + 1 = 3R(R+1) + 1 \tag{1}$$

In terms of user mobility model, two commonly used mobility models are taken into account: fluid-flow mobility model and random-walk mobility model. The fluid-flow model is more suitable for MNs with a high mobility and static speed/moving direction. On the other hand, the random-walk model is more appropriate for pedestrian movements where mobility is generally confined to a limited geographical area such as residential and business buildings [10].

2.1 Random Walk Mobility Model

In terms of random-walk mobility model, we use the one-dimensional Markov chain model used in [10]. In this model, the next position of an MN is equal to the previous position plus a random variable whose value is drawn independently from an arbitrary distribution. In addition, an MN moves to another cell area with a probability of $1 - q$ and remains in the current cell with probability, q. In the cellular architecture shown in Fig. 1, if an MN is located in a cell of ring r ($r > 0$), the probability that a movement will result in an increase ($p^+(r)$) or decrease ($p^-(r)$) in the distance from the center cell is given by

$$p^+(r) = \frac{1}{3} + \frac{1}{6r} \quad \text{and} \quad p^-(r) = \frac{1}{3} - \frac{1}{6r} \tag{2}$$

We define the state r of a Markov chain as the distance between the current cell of the MN and the center cell. This state is equivalent to the index of a ring where the MN is located. As a result, the MN is said to be in state r if it is currently residing in ring r. The transition probabilities $\alpha_{r,r+1}$ and $\beta_{r,r-1}$ represent the probabilities of the distance of the MN from the center cell increasing or decreasing, respectively. They are given as follows:

$$\alpha_{r,r+1} = \begin{cases} (1-q) & \text{if } r = 0 \\ (1-q)\left(\frac{1}{3} + \frac{1}{6r}\right) & \text{if } 1 \leq r \leq R \end{cases} \tag{3}$$

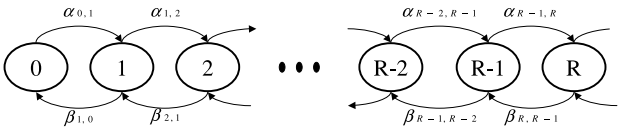

Fig. 2 State diagram for random walk mobility model.

$$\beta_{r,r-1} = (1-q)\left(\frac{1}{3} - \frac{1}{6r}\right) \quad \text{if } 1 \le r \le R \tag{4}$$

where q is the probability that an MN remains in the current cell.

Figure 2 shows a state transition diagram in the Markov chain for a random walk model. Let $\pi_{r,R}$ be the steady-state probability of state r within a MAP domain consisting of R rings. Using the transition probabilities in Eqs. (3) and (4), $\pi_{r,R}$ can be expressed in terms of the steady state probability $\pi_{0,R}$ as

$$\pi_{r,R} = \pi_{0,R} \prod_{i=0}^{r-1} \frac{\alpha_{i,i+1}}{\beta_{i+1,i}} \qquad \text{for } 1 \le \mathrm{r} \le \mathrm{R} \tag{5}$$

With the requirement $\sum_{\mathrm{r}=0}^{\mathrm{R}} \pi_{r,R} = 1$, $\pi_{0,R}$ can be expressed as

$$\pi_{0,R} = \frac{1}{1 + \sum_{r=1}^{R} \prod_{i=0}^{r-1} \frac{\alpha_{i,i+1}}{\beta_{i+1,i}}} \tag{6}$$

2.2 Fluid-Flow Mobility Model

Under the fluid-flow model, the direction of an MN's movement in a MAP domain is distributed uniformly in the range of $(0, 2\pi)$. v is the average velocity of an MN. Let R_c and R_d be cell crossing rate and MAP domain crossing rate, respectively. Therefore, the cell and domain crossing rates are as follows [9]:

$$R_c = \frac{\rho v L_c}{\pi} \tag{7}$$

$$R_d = \frac{\rho v L(R)}{\pi} \tag{8}$$

where L_c and $L(R)$ are the perimeters of a cell and a MAP domain consisting of R rings, respectively. v and ρ denote the average velocity and MN density, respectively. $L(R)$ can be obtained using the following equation.

$$L(R) = 6 \times (2R+1) \times \frac{L_c}{6} \qquad (R \ge 1) \tag{9}$$

3. Cost Functions

In cellular networks, there is a trade-off between location update cost and paging cost. Therefore, in order to analyze the performance of wireless/mobile networks, the total cost, consisting of location update cost and paging cost, should be considered. However, since HMIPv6 [6] does not support paging functions, we divide the total cost into *location update cost* and *packet delivery cost*. The location update cost and the packet delivery cost are denoted by $C_{location}$ and C_{packet}, respectively. Then, the total cost is the sum of location update cost and packet delivery cost.

$$C_{total} = C_{location} + C_{packet}$$

3.1 Location Update Cost

In HMIPv6, an MN performs two types of binding update procedures: *the global binding update* and *the local binding update*. The global binding update is a procedure in which an MN registers its RCoA with the CNs and the HA. On the other hand, if an MN changes its current address within a local MAP domain, it only needs to register the new address with the MAP. A local binding update refers to this registration. C_g and C_l denote the signaling costs in the global binding update and the local binding update, respectively. In the IP networks, the signaling cost is proportional to the distance of two network entities. Therefore, the signaling cost of the global binding update is larger than that of the local binding update. C_g and C_l can be obtained from the below equations.

$$\begin{aligned} C_g &= 2 \cdot (\kappa + \tau \cdot (D_{MAP-AR} + D_{HA-MAP})) \\ &\quad + 2 \cdot N_{CN} \cdot (\kappa + \tau \cdot (D_{MAP-AR} + D_{CN-MAP})) \\ &\quad + PC_{HA} + N_{CN} \cdot PC_{CN} + PC_{MAP} \\ C_l &= 2 \cdot (\kappa + \tau \cdot D_{MAP-AR}) + PC_{MAP} \end{aligned}$$

where τ and κ are the unit transmission costs in a wired and a wireless link, respectively. Let D_{CN-HA}, D_{HA-MAP}, D_{CN-MAP} and D_{MAP-AR} be the hop distance between the CN and the HA, the HA and the MAP, the CN and the MAP and the MAP and the AR, respectively. PC_{HA}, PC_{CN} and PC_{MAP} are the processing costs for binding update procedures at the HA, the CN and the MAP, respectively. N_{CN} denotes the number of CNs which are communicating with the MN.

3.1.1 Random Walk Mobility Model

According to the random mobility model proposed in the previous section, the probability that an MN performs a global binding update is as follows:

$$\pi_{R,R} \cdot \alpha_{R,R+1}$$

Specifically, if an MN is located in ring R, the boundary ring of a MAP domain composed of R rings, and performs a movement from ring R to ring $R+1$. The MN then performs the global binding update procedure. In other cases, except this movement, the MN only performs a local binding update procedure. Hence, the location update cost per unit time can be expressed as follows:

$$C_{location} = \frac{\pi_R \alpha_{R,R+1} C_g + (1 - \pi_R \alpha_{R,R+1}) C_l}{\overline{T}} \quad (10)$$

where $\overline{T}$ is the average cell residence time.

3.1.2 Fluid-Flow Mobility Model

In the previous section, the cell crossing rate (R_c) and domain crossing rate (R_d) in the fluid-flow model were obtained. The location update cost per MN can then be calculated as follows:

$$C_{location} = \frac{R_d \cdot C_g + (N_{AR} \cdot R_c - R_d) \cdot C_l}{\rho \cdot A(R)} \quad (11)$$

In Eq. (11), $A(R)$ refers to the area of a MAP domain. Let A_c be the area of a cell. The $A(R)$ can then be calculated as follows:

$$A(R) = N_{AR} \cdot A_c = N_{AR} \cdot \frac{\sqrt{3}}{24} \cdot L_c^2$$

where N_{AR} is the number of ARs in a MAP domain and $L_c^2 \cdot \sqrt{3}/24$ is the dimension of a hexagonal cell area. Since a MAP domain consists of multiple cells (i.e., N_{AR}) and the sum of all cell crossing rates in a MAP domain includes the MAP domain crossing rate, the overall rate performing a local binding update is $N_{AR} \cdot R_c - R_d$.

3.2 Packet Delivery Cost

Let N_{MN} be the total number of users located in a MAP domain. This paper assumes that the average number of users located in the coverage of an AR is K. Therefore, the total number of users can be obtained using Eq. (12).

$$N_{MN} = N_{AR} \times K \quad (12)$$

In case of the fluid-flow model, K is equal to $\rho \cdot A_c$.

The packet delivery cost (C_{packet}) in HMIPv6 can then be calculated as follows:

$$C_{packet} = C_{MAP} + C_{HA} + C_T \quad (13)$$

In Eq. (13), C_{MAP} and C_{HA} denote the processing costs for packet delivery at the MAP and the HA, respectively. C_T denotes the packet transmission cost from the CN to the MN.

In HMIPv6, a MAP maintains *a mapping table* for translation between RCoA and LCoA. The mapping table is similar to that of the HA, and it is used to track the current locations (LCoA) of the MNs. All packets directed to the MN will be received by the MAP and tunneled to the MN's LCoA using the mapping table. Therefore, the lookup time required for the mapping table also needs to be considered.

Specifically, when a packet arrives at the MAP, the MAP selects the current LCoA of the destination MN from the mapping table and the packet is then routed to the MN. Therefore, the processing cost at the MAP is divided into the lookup cost (C_{lookup}) and the routing cost ($C_{routing}$). The lookup cost is proportional to the size of the mapping table. The size of the mapping table is proportional to the number of MNs located in the coverage of a MAP domain. On the other hand, the routing cost is proportional to the logarithm of the number of ARs belonging to a particular MAP domain. Therefore, the processing cost at the MAP can be expressed as Eq. (14). In Eq. (14), λ_s denotes the session arrival rate and $\overline{S}$ denotes the average session size in the unit of packet. α and β are the weighting factors.

$$\begin{aligned} C_{MAP} &= \lambda_s \cdot \overline{S} \cdot (C_{lookup} + C_{routing}) \\ &= \lambda_s \cdot \overline{S} \cdot (\alpha N_{MN} + \beta \log(N_{AR})) \end{aligned} \quad (14)$$

In MIPv6, the route optimization is used to resolve the triangular routing problem. Therefore, only the first packet of a session transits the HA to detect whether or not an MN moves into foreign networks. Subsequently, all successive packets of the session are directly routed to the MN. The processing cost at the HA can be calculated as follows:

$$C_{HA} = \lambda_s \cdot \theta_{HA} \quad (15)$$

where θ_{HA} refers to a unit packet processing cost at the HA.

Unlike the processing cost, the transmission cost is associated with the distance between two network entities. In IP networks, the distance is represented as the number of hops. Since HMIPv6 supports the route optimization, the transmission cost in HMIPv6 can be obtained using Eq. (16). As mentioned before, τ and κ denote the unit transmission costs in a wired and a wireless link, respectively. In general, since the transmission cost in a wireless link is larger than that in a wired link, κ is larger than τ.

$$\begin{aligned} C_T &= \tau \cdot \lambda_s \cdot ((\overline{S} - 1) \cdot (D_{CN-MAP} + D_{MAP-AR}) \\ &\quad + (D_{CN-HA} + D_{HA-MAP} + D_{MAP-AR})) \\ &\quad + \kappa \cdot \lambda_s \cdot \overline{S} \end{aligned} \quad (16)$$

4. Numerical Results

This section presents various analysis results based on the developed analytic model. The parameter values for the analysis were referenced from [8] and [9]. They are shown in Table 1.

4.1 Location Update Cost vs. User Mobility

First, the impact of the user mobility on the location update cost is investigated. Figure 3 shows the variation in the location update cost as the average cell residence time is changed in the random-walk model. The MN performs fewer movements as the average residence time of an MN

Table 1 System parameters for numerical analysis.

α	β	θ_{HA}	τ	κ	PC_{HA}	PC_{MAP}	PC_{CN}	N_{CN}
0.1	0.2	20	1	2	24	12	6	2

D_{CN-HA}	D_{HA-MAP}	D_{CN-MAP}	D_{MAP-AR}	L_c
6	6	4	2	120 m

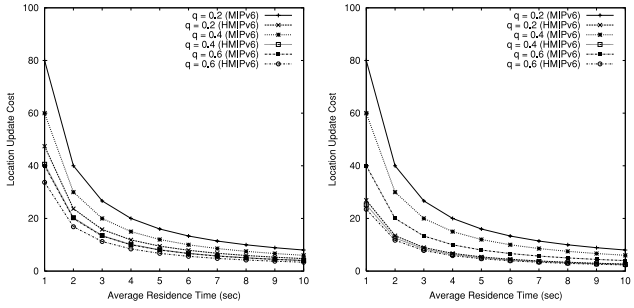

(a) R = 1 (b) R = 4

Fig. 3 Location update cost as a function of average residence time (Random-walk model).

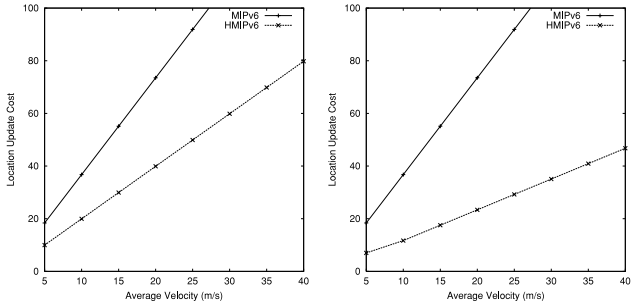

(a) R = 1 (b) R = 4

Fig. 4 Location update cost as a function of average velocity (Fluid-flow model).

increases. Therefore, the location update cost is inversely proportional to the average residence time. In addition, q denotes for the probability that an MN remains in the current cell at the next time unit. Therefore, MNs with a large q refer to static MNs. Namely, the MNs performs fewer movements and requires a lower location update cost. Besides, the location update cost of a ring with a size of 1 is larger than that of a ring with a size of 4, as shown in Fig. 3. This is because an MN located in the MAP domain with a small ring size is more likely to perform global binding update procedures. In a comparison of HMIPv6 with MIPv6, HMIPv6 requires only 59–84% (R=1) and 33–58% (R=4) of the location update cost in MIPv6. However, the gain in the HMIPv6 decreases as q increases.

On the other hand, Fig. 4 shows the location update cost as the MN's average velocity in the fluid-flow model. In this analysis, the user density is set as 0.0002. Since an MN with a higher average velocity has a higher domain crossing rate, a higher location update cost is required. Therefore, the location update cost increases as the average velocity increases. The signaling gain, which is defined as the location update cost of HMIPv6 to that of MIPv6, are 54% and 38% when R is 1 and 4, respectively.

In addition, the sensitivity of the location update cost to the variance in the cell residence time was investigated. It is assumed that the cell residence time follows a Gamma distribution. Equation (17) shows a probability density function of a Gamma distribution with a shape parameter k and

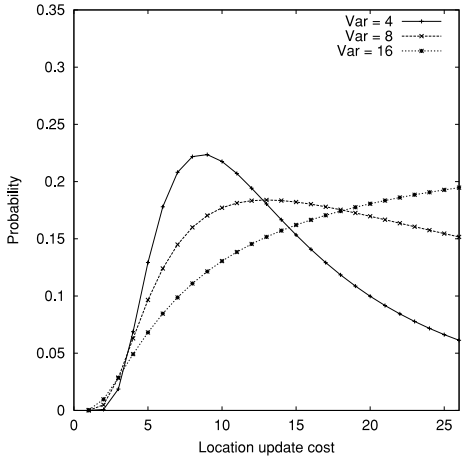

Fig. 5 The impact of variance in cell residence time.

a scale parameter b.

$$f_{gamma}(t) = \frac{1}{\Gamma(k) \cdot b^k} \mathrm{t}^{\mathrm{k}-1} \mathrm{e}^{-\mathrm{t}/\mathrm{b}} \tag{17}$$

where $\Gamma(k) = \int_0^\infty \mathrm{t}^{\mathrm{k}-1}\mathrm{e}^{-\mathrm{t}} dt$. The variance of the Gamma distribution is kb^2. Figure 5 is the probability distribution of the location update cost indicating the impact of the variance in a cell residence time. In this analysis, the average cell residence times are identical in the three cases ($\overline{T} = 4$). However, the variances are 4, 8, and 16, respectively. q is set to 0.4 and R is 3.

In terms of the average location update cost, since the average cell residence time is identical, the average location update costs for the three cases are same. However, different features can be identified from Fig. 5 when the variance of cell residence time is considered. In the cell residence time with a large variance, a high location update cost occupies a larger amount of the overall location update cost compared to the cell residence time with a small variance. This is because the probability that an MN will remains in a cell area for a shorter time increases as the variance of the cell residence time increases.

4.2 Packet Delivery Cost vs. User Population

In general, the location update cost is affected by the user mobility and not by the user population. In contrast, in case of a HMIPv6 without a paging function, the MAP needs to determine whether or not the destination MN belongs to the mapping table. The cost for this lookup procedure is generally proportional to the number of MNs in a MAP domain. Therefore, the packet delivery cost increases as the number of MNs in the MAP domain increases.

Figure 6 shows the impact of the number of MNs in an cell area on the packet delivery cost in a random-walk model. In this analysis, λ_s and $\overline{S}$ are equal to 0.1 and 10, respectively. As shown in Fig. 6, the packet delivery cost increases linearly as the number of MNs increases. This tendency is clearer in a larger MAP domain size. These re-

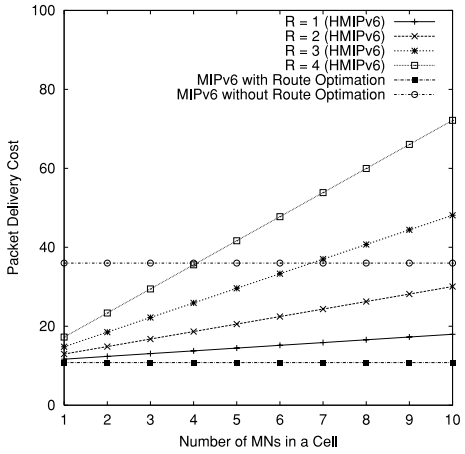

Fig. 6 Packet delivery cost as a function of the user population (Random-walk model).

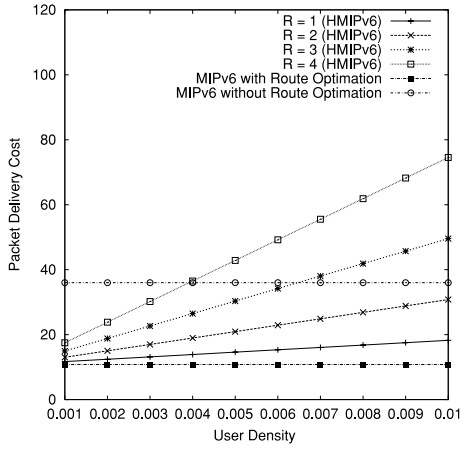

Fig. 7 Packet delivery cost as a function of the user density (Fluid-flow model).

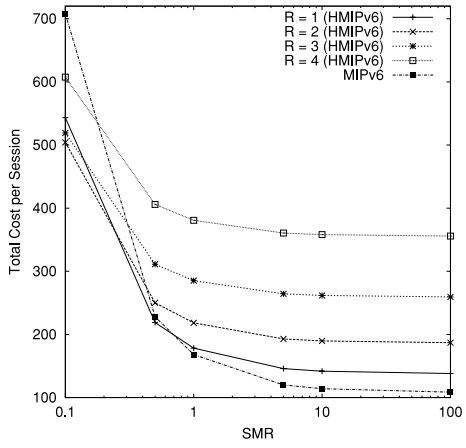

Fig. 8 Total cost vs. SMR (Random-walk model).

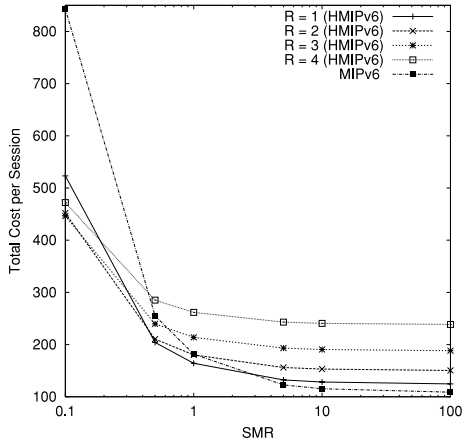

Fig. 9 Total cost vs. SMR (Fluid-flow model).

sults suggest that it is important to reduce the packet delivery cost for scalable services. In order to reduce the packet delivery cost, it is possible to minimize the lookup latency in a mapping table using efficient search algorithms. In terms of the comparison of HMIPv6 and MIPv6, the MIPv6 supporting route optimization has a lower packet delivery cost than HMIPv6 for all MAP domain sizes. This is because there is no processing cost at the MAP. However, MIPv6 without a route optimization procedure has a larger packet delivery cost than the HMIPv6 when there is a small number of MNs in a cell or the size of the MAP is small.

Figure 7 shows the packet delivery cost as the MN density (ρ) is changed in a fluid-flow model. The results shown in Fig. 7 are almost the same as those of Fig. 6

4.3 Total Cost vs. SMR

In this section, the total cost in HMIPv6 is analyzed. In order to do accomplish this, a performance factor called the session-to-mobility ratio (SMR), is defined. The SMR is analogous to the call-to-mobility ratio (CMR) used for the performance analysis in existing cellular networks. The SMR represents the relative ratio of the session arrival rate to the user mobility ratio. In the random-walk model, the SMR is defined as $\lambda_s \cdot \overline{T}$. On the other hand, the SMR in the fluid-flow model is equal to λ_s / R_c.

Using the SMR, the total cost per session is analyzed as the SMR is changed. Figures 8 and 9 show the total cost when the SMR is 0.1, 1, 10, and 100.

In Fig. 8, q and K are 0.4 and 4, respectively. When the SMR is 0.1, MIPv6 requires the largest total cost. However, when the SMR is larger than 1, it has the smallest total cost. This is because the packet delivery cost is the dominant factor when the session arrival rate is higher than the mobility ratio. This can be also found in Fig. 9, which shows the relationship between the total cost and the SMR in the fluid-flow model. In Fig. 9, the average velocity is 20 m/s and the user density is 0.0002.

In addition, Figs. 8 and 9 show the optimal MAP domain size as the SMR is changed. When the SMR is small, mobility rate is larger than the session arrival rate. Therefore, it is more important to reduce the location update cost than to reduce the packet delivery cost. Consequently, a large MAP domain size shows a smaller total cost. On the

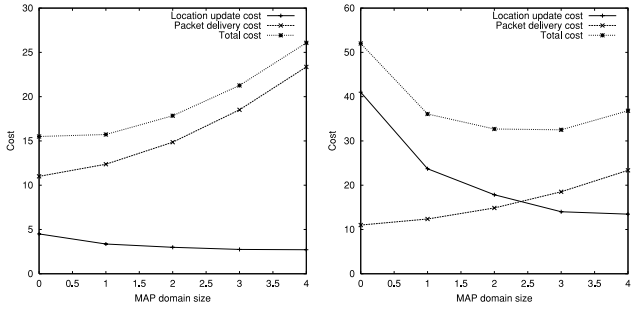

(a) Static MN (b) Dynamic MN

Fig. 10 Impact of user mobility on the total cost (Random-walk model).

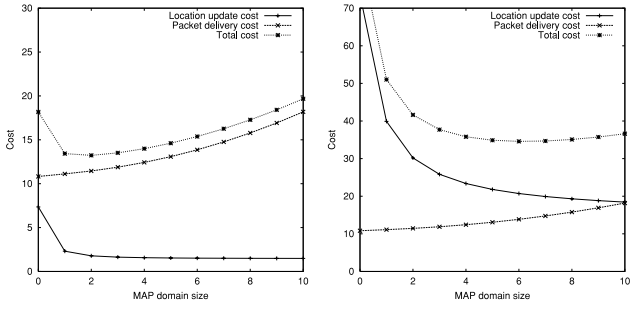

(a) Static MN (b) Dynamic MN

Fig. 11 Impact of user mobility on the total cost (Fluid-flow model).

other hand, if the session arrival rate is larger than the mobility rate (i.e., SMR is larger than 1), a large MAP domain shows a larger total cost due to a higher packet delivery cost. The next section investigates the optimal MAP domain size for the different user mobility types.

4.4 Optimal MAP Domain Size

In terms of network deployment, it is essential to determine the optimal MAP domain size minimizing the total cost. The tradeoff relationship between the location update cost and the packet delivery cost needs to be taken into account when determining the optimal MAP size. In this section, the optimal MAP domain size is examined as a function of different MNs. To characterize an MN's mobility, different parameter values, which affect the mobility, are used. In the case of the random-walk model, the static MN remains in the current cell with a probability of 0.8 and the average residence time is 8. In contrast, the dynamic MN remains in the current cell with a probability of 0.2 and the average residence time is 2. In the case of the fluid-flow model, the average velocities of the static and dynamic MNs are 2 m/s and 20 m/s, respectively. In addition, the user density is 0.0002.

Figure 10 shows the total cost for the static MN and dynamic MN in the random-walk model. In the case of the static MN, the location update cost is almost constant for all MAP domain sizes. This means that the packet delivery cost has an impact on the optimal MAP domain size because the location update cost does not change as the MAP domain size changes. Therefore, the optimal MAP domain size is 0 when the packet delivery cost is minimized. However, in the case of the dynamic MN, the location update cost decreases as the MAP domain size increases. Hence, in order to obtain the optimal MAP domain size, the MAP domain size required to minimize the total cost must be found. In the case of the dynamic MN presented in Fig. 10, the total cost is at a minimal when the ring size is 3, which is larger than the optimal MAP domain size of the static MN. Namely, the optimal MAP domain size increases as the user mobility increases.

Figure 11 shows the same analysis results in the fluid-flow model. The overall trend is similar to that of the random-walk model. The optimal value to minimize the total cost is 2 and 6 in static MN and dynamic MN, respectively. These results indicate that there is some benefit when enlarging the MAP domain size in the case of the dynamic MN. On the other hand, in the case of the static MN, a small MAP domain has the advantage of reducing the total cost.

5. Conclusion

Hierarchical Mobile IPv6 (HMIPv6) is a novel protocol designed to minimize the mobility-related signaling costs. In this paper, the location update cost and packet delivery cost in HMIPv6 was modeled using the random walk and fluid flow models. Using these models, the impact of cell residence time and user population on the location update cost and the packet delivery cost, respectively, was analyzed. In addition, the variation in the total cost was examined as the SMR and the MAP domain size are changed. The analysis results indicate that the MAP domain size and the SMR are critical performance factors in order to minimize the total cost in the HMIPv6. In addition, an efficient management scheme for the mapping table at the MAP is needed in order to reduce the lookup cost. In our future works, we will consider more different mobility models [12] such as group mobility model. Also, studies modeling and analyzing the HMIPv6 supporting IP paging, which has the advantages in minimization of the signaling overhead and power consumption, are currently underway.

Acknowledgement

This work was supported in part by the Brain Korea (BK) 21 project of the Ministry of Education and in part by the National Research Laboratory (NRL) project of the Ministry of Science and Technology, 2003, Korea.

References

[1] I.F. Akyildiz, J. Mcnair, J. Ho, H. Uzunalioglu, and W. Wang, "Mobility management in next-generation wireless systems," Proc. IEEE, vol.87, no.8, pp.1347–1384, Aug. 1999.

[2] IETF Mobile IP WG: http://www.ietf.org/html.charters/mobileip-charter.html

[3] C. Perkins, "IP mobility support for IPv4," IETF RFC 3344, Aug. 2002.

[4] D. Johnson, C. Perkins, and J. Arkko, "Mobility support in IPv6," IETF Internet draft, June 2002.

[5] E. Gustafsson, A. Jonsson, and C. Perkins, "Mobile IP regional registration," Internet Draft, draft-ietf-mobileip-reg-tunnel-02, Work in Progress, March 2000.
[6] C. Castelluccia and L. Bellier, "Hierarchical mobile IPv6," Internet Draft, draft-castelluccia-mobileip-hmipv6-00.txt, Work in Progress, July 2000.
[7] J. Xie and I.F. Akyildiz, "A distributed dynamic regional location management scheme for mobile IP," IEEE Trans. Mobile Computing, vol.1, no.3, pp.163–175, July 2002.
[8] M. Woo, "Performance analysis of mobile IP regional registration," IEICE Trans. Commun., vol.E86-B, no.2, pp.472–478, Feb. 2003.
[9] X. Zhang, J.G. Castellanos, and A.T. Capbell, "P-MIP: Paging extensions for mobile IP," ACM Mobile Networks and Applications, vol.7, no.2, pp.127–141, 2002.
[10] I.F. Akyildiz and W. Wang, "A dynamic location management scheme for next-generation multitier PCS systems," IEEE Trans. Wireless Commun., vol.1, no.1, pp.178–189, Jan. 2002.
[11] Y. Fang, "Movement-based mobility management and trade off analysis for wireless mobile networks," IEEE Trans. Comput., vol.52, no.6, pp.791–803, June 2003.
[12] T. Camp, J. Boleng, and V. Davies, "A survey of mobility models for ad hoc network research," Wireless Commun. and Mobile Computing (WCMC), vol.2, no.5, pp.483–502, 2002.

Sangheon Pack received B.S. (2000, magna cum laude) and M.S. (2002) degrees from Seoul National University, both in computer engineering. He is currently working toward a Ph.D. degree in the School of Computer Science and Engineering at the Seoul National University, Korea. He is a student member of the IEEE. Since 2002, he has been a recipient of the Korea Foundation for Advanced Studies (KFAS) Computer Science and Information Technology Scholarship. He has been also a member of Samsung Frontier Membership (SFM) from 1999. He received a student travel grant award for the IFIP Personal Wireless Conference (PWC) 2003. He was a visiting researcher to Fraunhofer FOKUS, German in 2003. His research interests include mobility management, QoS provision, and scalability issues in the next-generation wireless/mobile networks. Specifically, he is researching the performance of IP-based mobility protocols such as Mobile IP and IP-layer paging protocol.

Yanghee Choi received B.S. in electronics engineering from Seoul National University, M.S. in electrical engineering from Korea Advanced Institute of Science, and Doctor of Engineering in Computer Science from Ecole Nationale Superieure des Telecommunications (ENST) in Paris, in 1975, 1977 and 1984 respectively. Before joining the School of Computer Engineering, Seoul National University in 1991, he has been with Electronics and Telecommunications Research Institute(ETRI) during 1977–1991, where he served as director of Data Communication Section, and Protocol Engineering Center. He was research student at Centre National d'Etude des Telecommunications (CNET), Issy-les-Moulineaux, during 1981–1984. He was also Visiting Scientist to IBM T.J. Watson Research Center for the year 1988–1989. He is now leading the Multimedia Communications Laboratory in Seoul National University. He is also director of Computer Network Research Center in Institute of Computer Technology (ICT). He was editor-in-chief of Korea Information Science Society journals. He was chairman of the Special Interest Group on Information Networking. He has been associate dean of research affairs at Seoul National University. He was president of Open Systems and Internet Association of Korea. His research interest lies in the field of multimedia systems and high-speed networking.